Solvent debinding process in powder injection molding: experiments and numerical simulations

Belgacem Mamen, Thierry Barrière, Jean-Claude Gélin

Solvent debinding process in Powder Injection Molding: experiments and numerical simulations

Belgacem Mamen, Thierry Barrière, Jean-Claude Gelin

FEMTO-ST Institute, Applied Mechanics Department, ENSMM, CNRS UMR 6174, Besançon/ France, belgacem.mamen@femto-st.fr

Abstract. Powder Injection Molding (PIM) is a technology in which thermoplastic polymeric materials with a high content of metallic powders are molded in a required shape. In this paper, solvent debinding for copper green components shaped by powder injection molding has been investigated. All the solvent debinding process tests have been carried out in water at various temperatures [40 to 60°C]. The distribution of the remaining soluble binder content inside the specimen has been described by using second Fick's diffusion law. Numerical simulations based on the finite element method have been carried out for validation through determination of the remaining soluble binder content at different debinding times. Results also showed that solvent temperature and component thickness played a very important role in the water debinding process. A properly adapted model describing the required debinding time, for components with different thicknesses at different temperatures, has been established. The proposed numerical simulation model provides improved monitoring possibilities for solvent debinding process particularly to extract binder from the complicated molded components.

Keywords: solvent debinding process, copper green components, remaining soluble binder content, numerical modeling.

1. INTRODUCTION

Powder injection molding (PIM) is derived from the well known thermoplastic injection molding processes and uses fine metallic or ceramic powders compounded with polymer binders to shape green (micro) structured parts in a near net shaping process [1]. Because PIM is a binder-assisted forming technology, binder removal without loss of product integrity is a crucial point. The process of binder removal is generally called debinding [2].

The binder systems are classified by their debinding techniques and the more advanced debinding techniques require a two-step process, solvent debinding and thermal debinding process. During the first stage a lower molecular weight binder is dissolved into a fluid in order to create open pore channels within the metal powder assembly. These pore channels provide possibilities for the decomposed gas molecules of the remaining binders to escape to the compact surface during the second debinding step at high temperatures [3]. Solvent extraction, water debinding, and chemical degradation techniques are most common. A certain binder fraction remains rigid during the first step in order to provide mechanical strength during the chemical and physical removal of the main binder content. The amount of soluble binder removed during this step, should be great enough to form interconnected pores throughout the compact [4].

In the second processing step the remaining high molecular weight of binder system are removed using a properly adapted thermal treatment in a gas atmosphere (e.g., argon) well known as thermal debinding [5-6]. The advantage of the two-step binder systems is that the thermal binder fraction is greatly reduced, thus minimizing the risk of defects such as cracking and part deformation [7].

In the present paper, numerical simulations based on the finite element method have been carried out for validation through determination of the remaining soluble binder content at different debinding times. The effect of solvent temperature and component thickness during water debinding process has been investigated. The proposed numerical modeling provides improved monitoring possibilities for solvent debinding techniques particularly to extract binder from the complicated molded components numerically without any experimentation.

2. EXPERIMENTAL PROCEDURE

Copper powders with a pycnometer density of 8.5 g/cm^3 and an average oversize factor of 1.15, have been used as the base powder in this study. The feedstock has been prepared by polyMIM© in which copper powder has been mixed with a multicomponent binder system [8]. The chemical and physical characteristics of the polyMIM Cu999 [8] are listed in table 1.

After mixing, the feedstock has been injected using an injection press, in which square specimens (5.6×5.6×0.92mm) have been molded at 175°C. The square specimens are then debound at 40–60 °C with water as solvent. For measuring the soluble binder extraction rate, the specimens have been debound for different periods of time (15 min–2 h) and then dried at 40 °C for 24 h.

Table 1. Chemical and physical characteristics of the polyMIM Cu999 powders.

Composition	Cu	Balance
	Fe	0.1
	O	0.05
Density	8.58 g/cm3	
Yield strength Rp02	>50 Mpa	
Tensile strength Rm	>210 Mpa	
Hardness	>40 HB	

Figure 1 relates the temperature influence on the debinding process for square sample (5.6×5.6×0.92mm) at there different debinding temperatures. An increase in debinding temperature leads to an efficient improvement in debinding process, due to an improvement in solubility and diffusivity of soluble binder in water as function of temperature [9].

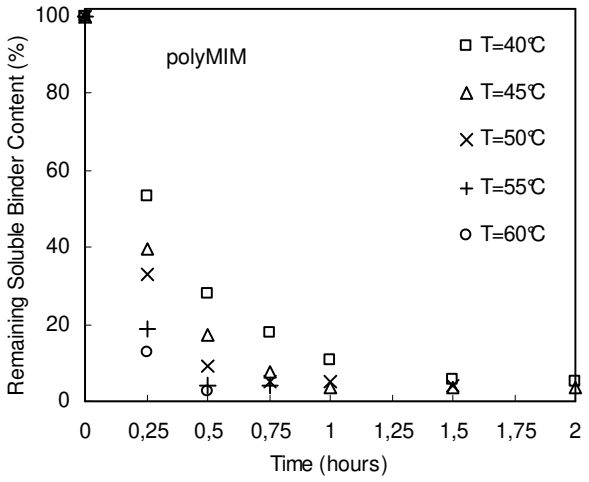

Figure 1. Binder remaining content inside 0.92-mm-thick square sample at different debinding temperatures from 40 to 60 °C.

An initially fast period followed by a progressively slower debinding rate can be observed for the five different debinding temperatures. During debinding process, water diffuses into PIM parts and then it occurs a reaction with soluble binder in order to dissolve it.

Figure 1 shows the binder remaining content for 0.92 mm thick polyMIM Cu999 at different debinding temperatures. The experimental results clearly show the influence of debinding temperature on the required debinding time. At 40°C, the samples reached 10 % of remaining binder after 1 hour in the water bath. Increasing the bath temperature to 50°C, the debinding time decreased to 0.5 hour. At a bath temperature 60°C, 10 % of remaining binder reached after 0.25 hour. One can say that the molecular mobility at 60°C is faster than 40°C which explain the short time obtained at 60°C and hence an increasing in water bath temperature leads automatically to an increase in removal rates.

Nevertheless, high temperatures are not recommended because the parts will lose their mechanical strength and deformations could occur.

3. MODELING AND NUMERICAL SIMULATION OF WATER DEBINDING

The solvent-debinding process can be considered as the interdiffusion of solvent and soluble binders within the specimen [10]. The distribution of the concentration (C) of the remaining soluble binder inside the specimen can be calculated by implanting second Fick's diffusion law, equation (1), in finite element software COMSOL®.

$$\frac{\partial C}{\partial t} = D\left(\frac{\partial^2 C}{\partial x^2} + \frac{\partial^2 C}{\partial y^2}\right) \quad \text{with} \quad D=\begin{bmatrix} D_{11} & 0 \\ 0 & D_{22} \end{bmatrix} \quad , D_{11} = D_{22} \qquad (1)$$

Initial conditions when t=0:

$C(x,0) = C_i, \quad and \quad -b \le x \le b$

$C(y,0) = C_i, \quad and \quad -a \le y \le a$

Boundary conditions when t>0:

$C(x,y,t)=C_0=0 \quad for \quad x=\pm b \quad and \quad y=\pm a$

$\frac{\partial C(x,t)}{\partial x}=0 \quad for \quad x=0 \quad and \quad \frac{\partial C(y,t)}{\partial y}=0 \quad for \quad y=0$

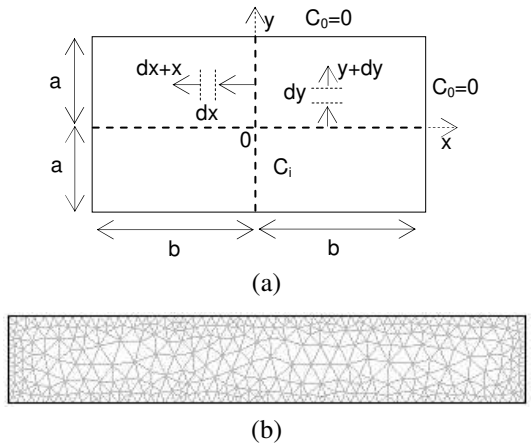

Figure 2. (a) Schematic of the diffusion model used in numerical simulation (b) Finite element discretization.

where t is the extraction time, *b* is the distance from the center plane of the specimen and is along the width direction, *a* is the distance from the center plane of the specimen and is along the thickness direction, D is the effective diffusion coefficient and C_0 is the boundary condition. The domain has been decretized using an automatic mesh generator with 668 triangular elements.

4. ANALYTICAL STUDY

The effective diffusion coefficient *D* must be analytically calculated using experimental data. Once *D* calculated one can solve equation (1) numerically using finite element code COMSOL Multiphysics®.

The analytical solution for a 1D approximation has been provided by Crank as [11]:

$$\frac{C_{rm}}{C_i} = \frac{4}{\pi}\sum_{n=0}^{\infty}\frac{(-1)^n}{(2n+1)}\exp\left(-D\frac{(2n+1)^2\pi^2}{4a^2}t\right)\times\cos\left(\frac{(2n+1)\pi y}{2a}\right) \qquad (2)$$

where C_i is the initial soluble binder content, C_{rm} is the average concentration of the remaining binder in the specimen.

For a long time debinding operation, equation (2) can be simplified as:

$$\frac{C_{rm}}{C_i} = \exp\left(-\frac{D\pi^2}{4a^2}t\right) \qquad (3)$$

Assuming *D* is only temperature-dependent, but not concentration-dependent:

$$D = D_0\exp\left(-\frac{E}{KT}\right) \qquad (4)$$

where D_0 is the pre-exponential frequency factor, *E* is the activation energy, *K* is the Boltzmann's constant and *T* is the temperature in K.

After a period of extraction, the binder concentration for the unidirectional diffusion could be approximated by substituting equation (4) into equation (3) that gives:

$$\ln\left(-\ln\frac{C_{rm}}{C_i}\right) = \ln\left(\frac{D_0\pi^2}{4a^2}t\right) + \frac{-E}{K}\frac{1}{T} \qquad (5)$$

A plot of ln (-ln (C_{rm}/C_i)) vs. 1/T is related in figure 3. From the linear regression analysis of this curve, the effective activation energy and then the diffusion coefficient for 0.92-mm-thick specimens can be obtained. For the specimen treated with a 30 minutes extraction, the amounts of soluble binder removed at 40°C, 45°C, 50°C, 55°C and 60°C were 27.8, 17.4, 9.2, 3.9 and 1.3 pct, respectively. The diffusion coefficient at 50°C, calculated from Eq. (5), was 1.13 310^{-10} m^2/s; the D_0 and E were 2.783 10^{-2} m^2/s and 51.88 kJ/mole, respectively.

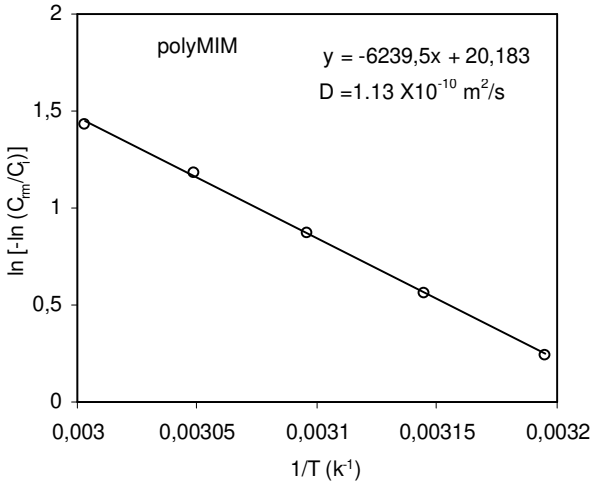

Figure 3. Temperature dependence of binder remaining after 30 min solvent debinding by linear regression fitting of equation (5).

5. RESULTS AND DISCUSION

Figure 4 shows a comparison between experimental and numerical remaining soluble binder content inside 0.92-mm-thick square sample at different debinding temperatures vs. time.

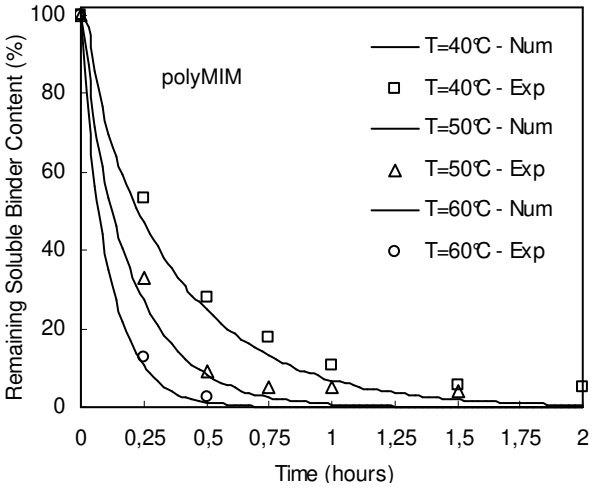

Figure 4. Comparison between experimental and numerical remaining soluble binder content inside 0.92-mm-thick square sample at different debinding temperatures from 40 to 60 °C.

It is shown that at the end of solvent debinding experiment, the amount of remaining soluble binder was slightly higher than the numerical value. This is due to a small amount of soluble binder which blended into the nonsoluble binder during mixing and could not be extracted during solvent debinding process. Other than these small differences, the experimental data are, in general, in proper agreement with the numerical simulation results. These results indicated that the proposed numerical simulation is accurate and can provide improved monitoring possibilities for solvent debinding techniques particularly to extract binder from the complicated molded components numerically without any experimentation.

The experimental data related in figure 4 shows that the maximal debinding amount of soluble binder is about 95%. This 95 pct, however, may increase as the amount of soluble binder in the binder system decreases, and vice versa. To reach this level of 95 pct, the debinding time needed for parts with different thicknesses at different temperatures is related in figure 5. One can notice that the debinding time increases with increased sample thickness and decreased debinding temperature. For example, when the thickness increases from 2.0 to 8.0 mm, the necessary debinding time will significantly increase, from 0.8 to 12.9 hours at 40°C and from 0.8 to 7 hours at 50°C. This study can thus provide a properly adapted model, related in equation (6), for PIM industries in selecting their required depending time.

$$t = \left(\frac{T_{\min}}{T} \right)^3 .e^2 \qquad (6)$$

where t is the required depending time in hours, T_{min} is the minimal debinding temperature that equal 40°C and T is the used debinding temperature and e is the component thickness in millimetres.

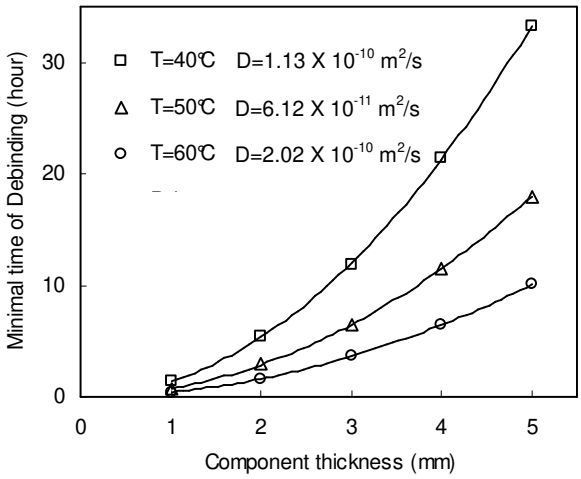

Figure 5. Debinding time needed to reach 95 % for components with different thicknesses at different temperatures.

Figure 6 illustrates the distribution of the remaining soluble binder after 5 minutes solvent debinding inside a 0.92-mm-thick square sample using 1D and 2D numerical simulations, respectively. During water solvent debinding the water molecules dissolve the soluble binder by starting from the component surface, the water penetrates gradually into the moulded sample as shown in figure 6. As the water diffuses into the component, it dissolves and extracts the soluble binder [12]. From this numerical

simulation, one can determine the amount of the remaining soluble binder inside the whole sample at any time.

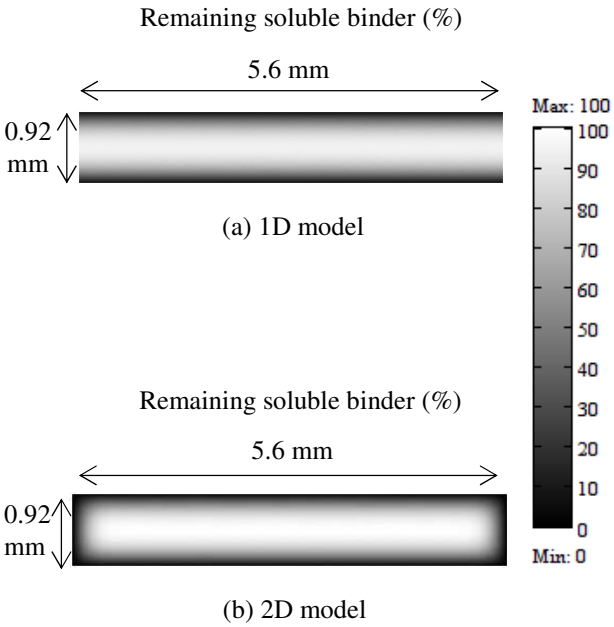

Figure 6. Contours of soluble binder content inside 0.92-mm-thick square sample after 5 minutes solvent debinding, (a) results for simulation 1D and (b) 2D.

In order to analyse the influence of width on the amount of remaining soluble binder, two tests have been conducted in 1D (y-direction) and 2D (both x and y-directions). Figure 7 shows the evolution of remaining soluble binder amount over time inside a component having 0.92-mm-thick and 5.6 mm in width. It is clearly shown that the width of the component has a little effect on the solvent debinding process in this study. One can conclude that the thickness plays a very important role in the water debinding process then the width one.

The 2D simulation is little faster than the 1D simulation. This is expected as the 1D simulation ignores lateral surfaces that soluble binder could escape from when compared with 2D simulation.

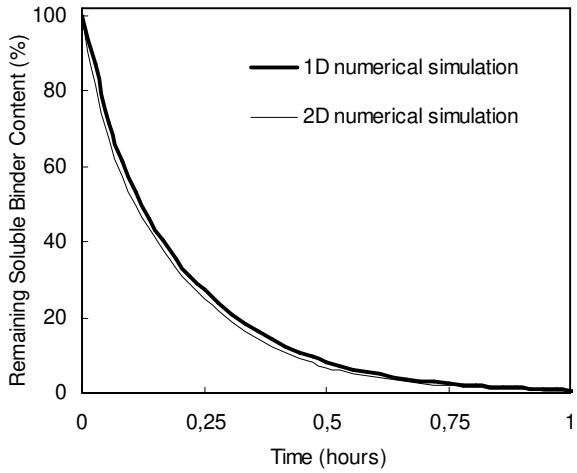

Figure 7. Binder remaining content inside 0.92-mm-thick square sample using 1D and 2D numerical simulations.

6. CONLUSIONS

In this paper, water debinding process for green copper components has been analysed. The remaining soluble binder content was found to follow a decreasing parabolic function of time and the final amount of remaining soluble binder was slightly higher than the numerical value. This is due to a small amount of soluble binder which was blended into the nonsoluble binder during mixing process and could not be extracted during solvent debinding process.

As demonstrated from the numerical simulation results, the binder dissolution started from the surface and progressed toward the center of the components. Therefore the distribution of the remaining soluble binder content inside the specimen can be determined at any processing time.

The debinding temperature and component thickness play a very important role in the water debinding process; a properly adapted model as a function of debinding temperature and component thickness has been established for PIM industries in order to select their solvent-debinding conditions.

The proposed numerical simulation is an accurate tool and provides improved monitoring possibilities for solvent debinding techniques particularly to extract binder from the complicated molded components numerically without any experimentation.

7. REFERENCES

[1] R.M. German, Powder injection molding, Metal Powder Industries Foundation, Princeton, New Jersey, (1990).

[2] G. Aggarwal, S.J. Park, I. Smid, R.M. German Metall: Master decomposition curve for binders used in Powder Injection Molding, Metall. Trans. A, 38 (2007), 606-714.

[3] Y.L. Fan, K.S. Hwang, S.H. Wu, Y.C. Liau: Minimum amount of binder removal required during solvent debinding of Powder Injection-Molded compacts, Metall. Trans. A, 40 (2009), 768-779.

[4] U.L Mohsin, D. Lager, C. Gierl, W. Hohenauer, H. Danninger: Simulation and optimisation for thermal debinding of copper MIM parts using thermokinetic analysis, Powder Metallurgy, 54 (2011), 30-35.

[5] B. Mamen, T. Barriere, J-C. Gelin: Study of the Thermal decomposition for different feedstocks Powder Injection Moulding, Euro PM2011, Barcelona, 3 (2011), 235-241.

[6] C. Quinard, J. Song, T. Barriere, J.C. Gelin, Elaboration of PIM feedstocks with 316L fine stainless steel powders for the processing o micro-components, Powder Technology, 208 (2011), 383-389.

[7] H. Angermann, Van der Biest: Binder removal in Powder Injection Molding, Reviews in Particulate Materials, 3 (1995), 35-69.

[8] E. Jochen, B. Dirk: Product specification-polyMIM®Cu999, (2009), Germany.

[9] V.B. Ricardo, S. Valdir, F. Marcio, P. Alfredo: Ceramic injection moulding: Influence of specimen dimensions and temperature on solvent debinding kinetics, Journal of Materials Processing Technology, 160 (2005), 213-220.

[10] W.W. Yang, K.Y. Yang, M.C. Wang, M.H. Hon: Solvent debinding mechanism for alumina injection molded compacts with water soluble binders, Ceram. Int. 29 (7) (2003), 745-756.

[11] J. Crank: The mathematics of diffusion, 2nd ed., Clarendon Press, Oxford, UK, (1975), 47–48.

[12] D. Auzene, S. Roberjot: Investigations into water soluble binder systems for PIM, PIM International, 5 (2011), 54-57.

Acknowledgements

The authors gratefully acknowledge the New PIM project members for funding this research through the FEMTO-ST Institute and ENSMM.